

Elasticity of Mafic Rocks from the Mid-Atlantic Ridge

Nikolas I. Christensen and George H. Shaw

(Received 1970 March 31)

Summary

Compressional wave velocities are reported to pressures of 10 kb for 57 cores of rock dredged from the Mid-Atlantic Ridge at 22° N and 4° S latitude. Shear wave velocities are reported to pressures of 10 kb for 9 rock cores. The rocks studied consist of basalt, altered basalt, dolerite and chlorite-rich greenstones. Compressional wave velocities for all of the rocks, with the possible exception of the dolerites, are similar to reported velocities of the oceanic crust over the Mid-Atlantic Ridge crest. None of the rocks appear to be abundant constituents of the oceanic layer (Layer 3). Relationships between bulk density and velocity are given at pressures of 0.4, 1, 2, 6 and 10 kb. The least squares solution at 10 kb, $V_p = 2.53\rho - 0.76$, falls between Birch's solutions for mean atomic weights 21 and 22.

Introduction

The most direct information available on the structure of the oceanic crust comes from marine seismic investigations. The seismic data are usually presented as models with layers of various thicknesses and velocities. Most reported velocities are for compressional waves, although a limited amount of data is available on shear velocity distributions. Average oceanic structure has been summarized by Hill (1957) and Raitt (1963). Refracted arrivals from the oceanic crust usually have four segments on a travel time-distance plot which represent three crustal layers and the upper mantle. The uppermost crustal layer (Layer 1) varies greatly in thickness and consists of unconsolidated or semiconsolidated sediments. This is underlain by basement (Layer 2, $V_p \sim 5 \text{ km s}^{-1}$) and the oceanic layer (Layer 3, $V_p \sim 6.7 \text{ km s}^{-1}$). The exact nature of layers 2 and 3 is still questionable.

According to the hypothesis of sea-floor spreading, mid-oceanic ridges are thought to be regions of oceanic crustal generation. Over the Mid-Atlantic Ridge layer 3 is absent from the axial zone (Le Pichon *et al.* 1965) and a thick section of layer 2 with a compressional wave velocity of 4.5 to 5.8 km s^{-1} lies directly upon mantle. Layer 3 is present, however, over the East-Pacific Rise (Raitt 1956). Over both ridge types total crustal thickness is less than normal.

The geologic implications of these seismic observations are highly debatable. Clearly a better understanding of oceanic ridge processes, including the generation of oceanic crust, depends upon reasonable estimates of oceanic crustal composition. The purpose of this paper is to present new laboratory data bearing on the interpretation of oceanic seismic refraction data in terms of mineral composition. Compressional and shear wave velocities are presented to pressures of 10 kb for several volcanics and low grade metamorphics dredged from the axial zone of the

Mid-Atlantic Ridge. The data are shown to have importance in placing limits on oceanic crustal composition and density.

Early investigations of elastic wave velocities at high pressures were usually limited to measurements of compressional waves in coarse grained igneous rocks. Velocities in granite were shown to be similar to upper continental crustal velocities, whereas velocities in gabbros were found to approximate velocities in the lower continental crust and the oceanic crust (Birch 1958). Thus the continental crust was commonly referred to as granitic and gabbroic and the oceanic crust was believed to be gabbroic (e.g., Gutenberg 1955, 1959). Recently several papers have reported compressional wave velocities at elevated pressures for a wider variety of plutonic igneous rocks and several metamorphic rocks (Birch 1960, 1961; Kanamori & Mizutani 1965; Christensen 1965, 1966b, 1970). Samples in these studies were obtained from continental areas. Compressional wave velocities also have been measured in a variety of basalts (Christensen 1968; Manghnani & Woollard 1968). These measurements show that crustal velocities which were interpreted as suggestive of granite or gabbro can also be explained by the presence of metamorphic and volcanic rocks.

Shear velocities at elevated pressures have been measured in several continental plutonic igneous rocks and metamorphic rocks (Simmons 1964; Kanamori & Mizutani 1965; Christensen 1966a, 1966b). No data have been published for basic volcanics or their low grade metamorphic equivalents, greenstones. The shear wave velocity data, when combined with compressional wave velocities, can be used to calculate the elastic constants of rocks under the assumption of isotropic elasticity. These constants provide additional important parameters which, when compared to elastic constants of the oceanic crustal layers, can further place limitations on crustal composition.

Notation

V_p ,	compressional wave velocity, km s^{-1}
V_s ,	shear wave velocity, km s^{-1} .
ρ_b ,	bulk density, g cm^{-3} .
ρ_p ,	particle density, g cm^{-3} .
β ,	compressibility, Mb^{-1} .
λ ,	Lamé's constant, Mb.
μ ,	shear modulus, Mb.
σ ,	Poisson's ratio.
ϕ ,	seismic parameter, $(\text{km s}^{-1})^2$.
E ,	Young's modulus, Mb.
K ,	bulk modulus, Mb.

Description of specimens

The rocks in this study with the prefix W were dredged on the crest and in the median valley of the Mid-Atlantic Ridge between 22° and 23° N in 1965 on cruise 1965-1 of R. V. *Thomas Washington*. The area was first examined during cruise 44 of R. V. *Chain* (van Andel *et al.* 1965; Melson & van Andel, 1966; van Andel & Bowin 1968). Melson *et al.* (1968) have studied in detail the petrology and chemistry of the rocks obtained on cruise 1965-1 of R. V. *Thomas Washington*. Locations of the dredged slopes where the samples in the present study were collected are shown in Fig. 1 of Melson *et al.* (1968).

The basalt samples were cored from massive fragments and pillows and consist primarily of plagioclase, subcalcic augite, olivine, titanomagnetite, and ilmenite. Volcanic glass and various products of deuteric alteration are common. Chemical analyses of pillow lavas and massive, holocrystalline basalts from this area (Melson *et al.* 1968, p. 5930) show little variation in composition. Chemically the basalts are oceanic tholeiites with compositions similar to previously reported chemical analyses of fresh basalts dredged from or near the Mid-Atlantic Ridge.

The dolerites are similar in mineralogy to the basalts. Some deuteric alteration is common in all the samples included in the present study. A chemical analysis of a dolerite collected on the *Chain 44* cruise (Melson *et al.* 1968, p. 5933) is similar to the basalts, with the exception of slightly higher Al_2O_3 in the dolerite. Estimated modes of the basalts and dolerites are given in Table 1.

Petrography and chemistry of greenstones collected between 22° and 23° N are given by Melson *et al.* (1968). The samples included in our study have not undergone the extensive mineralogical reconstitution of many of the greenstones reported from the same area by Melson & van Andel (1966). The samples, which are mylonitized and brecciated, consist primarily of chlorite along with relic augite and plagioclase. Melson *et al.* (1968) interpreted these greenstones to have originated by hydrothermal activity rather than regional metamorphism.

The greenstones with the prefix A were collected from the Mid-Atlantic Ridge at 4° S on Cruise 42 of *Atlantis II*. The samples are highly brecciated and are similar in mineralogy to the greenstones from the Mid-Atlantic Ridge at 22° N. The petrology of samples from this area has been reported by Thompson *et al.* (1969).

Experimental method

The velocities are obtained by measuring the transit times of compressional and shear waves in cylinders of rocks. Details of this technique are described by Birch (1960). The rock cores, 1.3 to 2.5 cm in diameter and 3.0 to 5.3 cm in length, are jacketed with copper foil to exclude the pressure medium from the pore spaces of the rocks. The ends of the cores are painted with silver conducting paint. Barium titanate and AC-cut quartz transducers with natural resonance frequencies of 2 MHz are used to generate compressional and shear waves respectively. The transducers are cemented with silver conducting epoxy to aluminium electrodes and held against the core ends by rubber tubing. The tubing excludes the pressure medium from the transducer-rock interface and the unjacketed core ends.

Table 1

Modal analyses, percentages by volume

Identification Number	Plagioclase	Pyroxene	Olivine	Opaques	Others*	Plagioclase composition, % Anorthite
W-2-8	50	25	—	10	15	57
W-4-115	47	14	3	10	26	52
W-8-2	56	34	—	7	3	38-69
W-9-78	40	9	1	20	30	67
W-7-1	50	31	1	10	8	60
W-2-6	55	30	—	7	8	57
W-4-427	46	29	4	11	10	49
W-2-4	39	28	—	8	25	56
W-14-442	35	30	2	15	18	57
W-4-15	40	10	—	20	30	68
W-10-2	61	29	—	3	7	36-55
W-10-1	50	34	1	7	8	58
W-10-3	51	31	—	7	11	53

* Principally alteration products and glass

A pulse of approximately 50 volts from a Hewlett Packard 214A pulse generator excites one of the transducers. The pulse from the driving transducer passes through the sample and is converted into an electrical signal by the receiving transducer which is amplified and displayed on a dual trace oscilloscope. Simultaneously, the pulse excites a transducer at one end of a variable length mercury delay line. The signal through the mercury is received by a second transducer, amplified and displayed on the second trace of the oscilloscope. By varying the distance between the transducers in the mercury delay line, the two signals on the oscilloscope can be superimposed. The delay line is calibrated with steel standards to produce equivalent travel times through the mercury column and the specimen when the signals are superimposed on the oscilloscope screen. The velocity in the rock is calculated from the length of the core, the length of the mercury column, and the velocity of mercury.

The pressure system is capable of generating pressures to 10 kb at room temperature in a cavity 3.5 cm in diameter and 15.2 cm long. The system utilizes a two stage pumping technique with a pressure intensifier. The high pressure fluid used is plexsol, produced by Esso Corporation. Pressure is measured by means of a manganin coil which is accurate to ± 1 per cent.

The error in the velocity determinations is due to a number of sources: the length of the sample, the effect of temperature on the velocity in mercury, uncertainties in the calibration of the delay line, and most important, the uncertainty in superimposing the signals from the sample and the delay line. This last source of error is greater for shear wave velocities than for compressional wave velocities and is expressed as an uncertainty in the length of the mercury column. The length of the sample is determined by means of a vernier caliper or micrometer. The per cent error in the length is about 0.1 per cent. The error due to the temperature effect on the velocity in mercury is approximately 0.2 per cent. For compressional velocity determinations the error in the length of the mercury column is approximately 0.2 per cent and for shear waves this error is about 0.5 per cent. Thus the limits of error for compressional and shear velocities are estimated roughly to be 0.5 per cent and 1.0 per cent respectively.

Data

Compressional and shear wave velocities for the rocks are given in Tables 2 and 3. Bulk densities on Table 2 were obtained from the weights and dimensions of the cylindrical samples. Particle densities were calculated from the weights and volumes of pulverized specimens. Shear velocities are reported for representative samples of each rock type. The velocities in Tables 2 and 3 have not been corrected for change in length due to compression. This correction lowers 10 kb velocities by approximately 1 per cent (Birch 1960). Earlier studies have shown that it is important to establish the degree of anisotropy in rocks (Birch 1961; Christensen 1965, 1966a), especially when elastic constants are calculated from velocity data. Thus for most specimens, velocities are reported for three perpendicular cores.

Velocities recorded with increasing pressure are usually slightly lower than velocities obtained with decreasing pressure. For a few of the basalts the reverse effect was observed for compressional wave velocities at low pressures. This has also been reported for basalts from Hawaii (Manghnani & Woollard 1968) and is illustrated in Fig. 1 for a specimen of basalt. Velocities reported in Tables 2 and 3 are simple averages of measurements taken with increasing and decreasing pressure. The initial rapid increase of velocity with increasing pressure (Fig. 1) is due to closure of grain boundary cracks (Birch 1960). At pressures above a few kilobars the cracks are closed and the velocities show a relatively small increase with further increase in pressure.

Table 2
Compressional wave velocities (km s^{-1})

ROCK	Identification number	Bulk density	Particle density	$p = 0.20 \text{ kb}$	$p = 0.40 \text{ kb}$	$p = 0.60 \text{ kb}$	$p = 0.80 \text{ kb}$	$p = 1.0 \text{ kb}$	$p = 2.0 \text{ kb}$	$p = 4.0 \text{ kb}$	$p = 6.0 \text{ kb}$	$p = 8.0 \text{ kb}$	$p = 10.0 \text{ kb}$
Greenstone	A-II-42-1-3-1	2.746		5.547	5.647	5.723	5.770	5.798	5.928	6.083	6.175	6.232	6.265
	A-II-42-1-3-2	2.695		5.397	5.595	5.685	5.749	5.799	5.928	6.083	6.175	6.232	6.265
Mean	A-II-42-1-3-3	2.627	2.889	4.866	5.056	5.134	5.199	5.242	5.403	5.600	5.731	5.815	5.866
Greenstone	A-II-42-1-4-1	2.688		5.270	5.433	5.514	5.573	5.613	5.753	5.922	6.027	6.093	6.132
	A-II-42-1-4-2	2.708		5.223	5.353	5.431	5.486	5.510	5.618	5.767	5.856	5.910	5.940
Mean	A-II-42-1-4-3	2.728	2.936	5.378	5.514	5.586	5.662	5.700	5.811	5.989	6.038	6.087	6.111
Greenstone	W-2-3	2.708		5.552	5.659	5.705	5.748	5.780	5.870	5.982	6.065	6.117	6.148
	W-2-3-Ia	2.721		5.384	5.509	5.574	5.632	5.663	5.766	5.903	5.986	6.038	6.066
	W-2-3-I	2.704		5.033	5.169	5.251	5.326	5.351	5.510	5.720	5.850	5.938	5.990
	W-2-3-II	2.733		4.832	5.002	5.124	5.210	5.256	5.445	5.674	5.818	5.908	5.960
	W-2-3-III	2.712		4.861	4.967	5.055	5.147	5.197	5.378	5.598	5.734	5.818	5.863
Mean		2.717	2.831	4.983	5.118	5.219	5.301	5.340	5.553	5.797	5.940	6.038	6.097
Basalt (altered)	W-2-8-I	2.778		4.701	4.829	4.927	5.014	5.067	5.254	5.490	5.625	5.700	5.740
	W-2-8-II	2.749		4.882	5.017	5.115	5.200	5.242	5.428	5.656	5.793	5.880	5.930
	W-2-8-III	2.753		4.904	5.056	5.185	5.280	5.335	5.550	5.847	5.992	6.089	6.155
Mean		2.760	2.902	4.881	5.050	5.164	5.251	5.302	5.548	5.830	5.973	6.068	6.130
Basalt (altered)	W-4-115-II	2.724		4.819	4.988	5.093	5.177	5.228	5.510	5.798	5.953	6.052	6.120
	W-4-115-III	2.843		5.474	5.531	5.591	5.652	5.662	5.860	6.035	6.128	6.180	6.207
Mean		2.784	2.926	5.616	5.650	5.687	5.740	5.755	5.916	6.070	6.154	6.203	6.230
Basalt	W-8-2-II	2.762		5.613	5.711	5.812	5.879	5.937	6.138	6.313	6.395	6.430	6.440
	W-8-2-III	2.808		5.514	5.700	5.815	5.920	5.966	6.178	6.343	6.407	6.430	6.440
Mean		2.785	2.973	5.564	5.706	5.814	5.900	5.952	6.158	6.328	6.401	6.430	6.440
Greenstone	W-2-1-I	2.805		5.696	5.764	5.801	5.830	5.847	5.920	6.020	6.093	6.155	6.207
	W-2-1-II	2.810		5.886	5.924	5.957	5.983	5.991	6.070	6.165	6.228	6.282	6.328
Mean		2.808	2.918	5.791	5.844	5.879	5.907	5.919	5.995	6.093	6.161	6.219	6.268
Basalt (altered)	W-9-78-I	2.787		5.545	5.687	5.796	5.864	5.937	6.160	6.349	6.418	6.462	6.487
	W-9-78-II	2.855		6.090	6.150	6.193	6.238	6.267	6.374	6.484	6.542	6.578	6.598
	W-9-78-III	2.803		4.760	5.053	5.239	5.469	5.596	6.080	6.375	6.485	6.548	6.554
Mean		2.815	2.968	5.465	5.630	5.743	5.856	5.933	6.205	6.403	6.482	6.529	6.546

Table 2 (continued)

ROCK	Identification number	Bulk density	Particle density	p = 0.20 kb	p = 0.40 kb	p = 0.60 kb	p = 0.80 kb	p = 1.0 kb	p = 2.0 kb	p = 4.0 kb	p = 6.0 kb	p = 8.0 kb	p = 10.0 kb
Basalt	W-7-1-I	2.861		5.932	5.976	6.004	6.036	6.058	6.154	6.247	6.289	6.312	6.316
	W-7-1-II	2.823		4.834	5.116	5.308	5.488	5.599	6.012	6.315	6.430	6.473	6.488
Mean	W-7-1-III	2.807	2.977	5.585	5.726	5.813	5.895	5.946	6.110	6.270	6.335	6.362	6.367
		2.830		5.450	5.606	5.708	5.806	5.868	6.092	6.277	6.351	6.382	6.389
Greenstone	W-2-10-I	2.846		6.076	6.104	6.127	6.143	6.155	6.229	6.318	6.377	6.427	6.463
	W-2-10-II	2.812		5.983	5.990	6.038	6.059	6.077	6.153	6.275	6.358	6.427	6.483
Mean	W-2-10-III	2.857		5.901	5.938	5.956	5.987	6.007	6.093	6.220	6.285	6.324	6.348
		2.838	2.965	5.987	6.011	6.040	6.063	6.080	6.158	6.271	6.340	6.393	6.431
Basalt	W-2-6-I	2.841		5.886	5.968	6.021	6.069	6.105	6.231	6.379	6.460	6.504	6.523
	W-2-6-II	2.837		5.730	5.806	5.892	5.944	5.984	6.126	6.288	6.380	6.438	6.468
Mean	W-2-6-III	2.835		5.734	5.809	5.879	5.936	5.977	6.112	6.273	6.366	6.423	6.450
		2.838	2.946	5.783	5.861	5.931	5.983	6.022	6.156	6.313	6.402	6.455	6.480
Basalt	W-4-427-I	2.824		5.728	5.820	5.891	5.969	6.009	6.188	6.350	6.420	6.450	6.462
	W-4-427-II	2.854		5.788	5.845	5.908	5.971	6.004	6.153	6.305	6.378	6.405	6.410
Mean	W-4-427-III	2.846		5.604	5.704	5.781	5.859	5.911	6.110	6.305	6.395	6.434	6.443
		2.841	2.890	5.707	5.790	5.860	5.933	5.975	6.150	6.320	6.398	6.430	6.438
Basalt (altered)	W-2-4-I	2.878		6.106	6.139	6.163	6.183	6.184	6.252	6.358	6.428	6.470	6.495
	W-2-4-II	2.835		5.836	5.870	5.903	5.936	5.946	6.033	6.169	6.260	6.316	6.353
Mean	W-2-4-III	2.847		5.889	5.908	5.933	5.967	5.986	6.083	6.212	6.300	6.362	6.405
		2.853	2.917	5.944	5.972	6.000	6.029	6.039	6.123	6.246	6.329	6.383	6.418
Greenstone	W-2-2-A	2.812		5.622	5.681	5.721	5.750	5.763	5.853	5.990	6.085	6.150	6.190
	W-2-2-B	2.833		5.864	5.890	5.916	5.941	5.951	6.030	6.135	6.207	6.253	6.285
	W-2-2-I	2.863		6.160	6.187	6.207	6.220	6.234	6.300	6.400	6.465	6.510	6.533
Mean	W-2-2-III	2.917		6.014	6.041	6.057	6.073	6.089	6.138	6.215	6.268	6.307	6.336
		2.856	2.939	5.915	5.950	5.975	5.996	6.009	6.080	6.185	6.226	6.305	6.336
Basalt (altered)	W-14-442-A	2.881		5.834	5.929	6.011	6.081	6.129	6.325	6.510	6.582	6.606	6.612
	W-14-442-B	2.836		5.995	6.060	6.112	6.144	6.166	6.300	6.457	6.519	6.543	6.550
Mean	W-14-442-C	2.855		5.848	5.921	5.963	6.011	6.038	6.183	6.340	6.417	6.447	6.457
		2.857	2.966	5.892	5.970	6.029	6.079	6.111	6.269	6.436	6.506	6.532	6.540
Basalt (altered)	W-4-15-I	2.864		5.708	5.963	6.143	6.251	6.303	6.422	6.543	6.589	6.605	6.608
	W-4-15-II	2.845		5.334	5.497	5.668	5.816	5.910	6.300	6.473	6.540	6.567	6.577
Mean	W-4-15-III	2.869		5.359	5.760	5.892	6.057	6.098	6.335	6.518	6.594	6.628	6.640
		2.859	2.969	5.467	5.743	5.901	6.041	6.104	6.352	6.511	6.574	6.600	6.608

Dolerite	W-10-2-A	2·877	6·146	6·198	6·227	6·249	6·256	6·328	6·421	6·485	6·522	6·545
	W-10-2-B	2·883	6·117	6·160	6·191	6·220	6·240	6·312	6·417	6·487	6·528	6·550
Mean	W-10-2-C	2·873	6·108	6·151	6·188	6·217	6·224	6·322	6·442	6·522	6·567	6·580
		2·878	2·950	6·170	6·202	6·229	6·240	6·321	6·427	6·498	6·539	6·558
Dolerite	W-10-1-I	2·882	5·861	5·902	5·950	5·971	5·983	6·112	6·260	6·352	6·410	6·452
	W-10-1-II	2·870	5·934	5·977	5·993	6·047	6·068	6·179	6·315	6·400	6·453	6·480
Mean	W-10-1-III	2·907	5·959	6·008	6·043	6·063	6·089	6·187	6·318	6·397	6·456	6·498
		2·886	2·997	5·918	5·995	6·027	6·047	6·159	6·298	6·383	6·440	6·477
Dolerite	W-10-3-I	2·893	5·840	5·889	5·927	5·963	5·986	6·118	6·274	6·358	6·407	6·437
	W-10-3-II	2·897	5·825	5·871	5·919	5·945	5·972	6·100	6·269	6·365	6·410	6·425
Mean	W-10-3-III	2·887	5·920	5·966	6·006	6·037	6·056	6·150	6·276	6·347	6·385	6·400
		2·892	2·966	5·909	5·951	5·982	6·005	6·123	6·273	6·357	6·401	6·421

Table 3

Shear wave velocities (km s^{-1})

ROCK	Identification number	$p = 0.20 \text{ kb}$	$p = 0.40 \text{ kb}$	$p = 0.60 \text{ kb}$	$p = 0.80 \text{ kb}$	$p = 1.0 \text{ kb}$	$p = 2.0 \text{ kb}$	$p = 4.0 \text{ kb}$	$p = 6.0 \text{ kb}$	$p = 8.0 \text{ kb}$	$p = 10.0 \text{ kb}$
Greenstone	W-2-10-I	3·178	3·188	3·198	3·205	3·214	3·249	3·290	3·314	3·327	3·330
	W-2-10-II	3·246	3·261	3·275	3·289	3·300	3·341	3·409	3·434	3·448	3·455
Mean	W-2-10-III	3·175	3·185	3·194	3·202	3·209	3·240	3·282	3·313	3·339	3·359
		3·200	3·211	3·222	3·232	3·241	3·277	3·327	3·353	3·371	3·381
Basalt (altered)	W-4-15-I	3·280	3·390	3·456	3·500	3·522	3·587	3·645	3·667	3·676	3·680
	W-4-15-II	3·130	3·242	3·315	3·375	3·402	3·527	3·620	3·651	3·660	3·663
Mean	W-4-15-III	3·100	3·220	3·305	3·366	3·410	3·543	3·641	3·672	3·684	3·688
		3·170	3·284	3·359	3·414	3·445	3·552	3·635	3·663	3·673	3·677
Dolerite	W-10-2-A	3·470	3·492	3·513	3·523	3·550	3·628	3·725	3·775	3·803	3·820
	W-10-2-B	3·559	3·575	3·588	3·602	3·615	3·662	3·721	3·755	3·775	3·792
Mean	W-10-2-C	3·614	3·625	3·636	3·647	3·656	3·697	3·753	3·787	3·812	3·825
		3·548	3·564	3·579	3·594	3·607	3·662	3·733	3·772	3·797	3·812

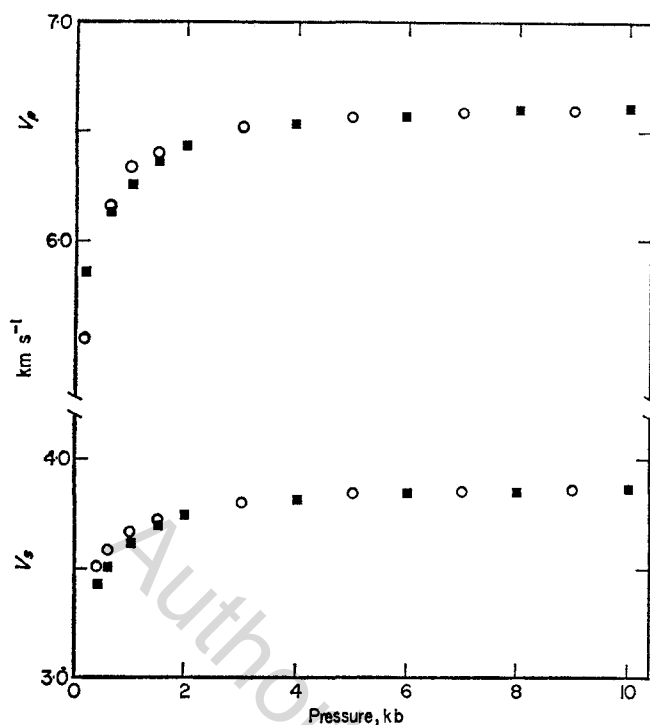


FIG. 1. Compressional and shear wave velocities for a specimen of basalt (W-4-15-I) as a function of pressure. Dots indicate measurements with increasing pressure; circles, with decreasing pressure.

The data in Tables 2 and 3 are for partially water saturated specimens. Several recent studies (e.g., Dortman & Magid 1969; Nur & Simmons 1969) have shown that the degree of water saturation can have a large effect on compressional wave velocities below a few kilobars. Comparisons of saturated and dry velocities in these studies represent rather extreme conditions which are probably not completely applicable to rocks in the Earth's crust. The dry velocities are usually measured from samples which have been heated to drive off any free water between grain boundaries. This heating, in addition to driving off water, tends to loosen the grain structure which, in turn, may produce a drop in low pressure velocities. Complete water saturation is usually accomplished by immersing the samples in water within a vacuum chamber.

The effect of water saturation on the volcanics and low grade metamorphics is usually much less than that observed for coarse grained igneous rocks. Presumably this behaviour may indicate less connected void space. Compressional wave velocities at pressures between 0.2 and 0.4 kb for completely saturated Mid-Atlantic Ridge specimens show an average increase of 4 per cent over the velocities reported in Table 2. At pressures above a few kilobars the velocity difference is within the error of measurement.

The elastic constants given in Table 4 were calculated at five pressures for the three rocks for which both compressional and shear wave velocities were determined. They were calculated from the measured values of V_p , V_s and ρ_b assuming isotropic elasticity. Corrections were made for compression using an iterative routine and the dynamically determined compressibility. The estimates of error in the elastic constants were determined from the estimated errors in the velocities and the error in the

Table 4

Elastic constants calculated from V_p , V_s , and ρ_b

Pressure, kb	V_p/V_s	σ	ϕ (km s^{-1}) ²	K , Mb	β , Mb^{-1}	μ , Mb	E , Mb	λ , Mb
Dolerite, W-10-2								
0.4	1.73	0.25	21.1	0.61	1.64	0.37	0.91	0.36
1.0	1.73	0.25	21.6	0.62	1.61	0.37	0.94	0.37
2.0	1.73	0.25	22.0	0.64	1.57	0.39	0.96	0.39
6.0	1.72	0.25	23.1	0.67	1.49	0.41	1.02	0.40
10.0	1.72	0.25	23.4	0.68	1.46	0.42	1.05	0.40
Altered basalt, W-4-15								
0.4	1.75	0.26	18.6	0.53	1.88	0.31	0.77	0.33
1.0	1.77	0.27	21.4	0.61	1.63	0.34	0.86	0.39
2.0	1.79	0.27	23.5	0.67	1.49	0.36	0.92	0.43
6.0	1.79	0.27	25.2	0.73	1.38	0.38	0.98	0.47
10.0	1.80	0.28	25.4	0.74	1.36	0.39	0.99	0.48
Greenstone, W-2-10								
0.4	1.87	0.30	22.4	0.64	1.57	0.29	0.76	0.44
1.0	1.88	0.30	22.9	0.65	1.53	0.30	0.78	0.45
2.0	1.88	0.30	23.6	0.67	1.49	0.31	0.79	0.47
6.0	1.89	0.31	25.1	0.72	1.39	0.32	0.84	0.50
10.0	1.90	0.31	26.5	0.74	1.35	0.32	0.84	0.52

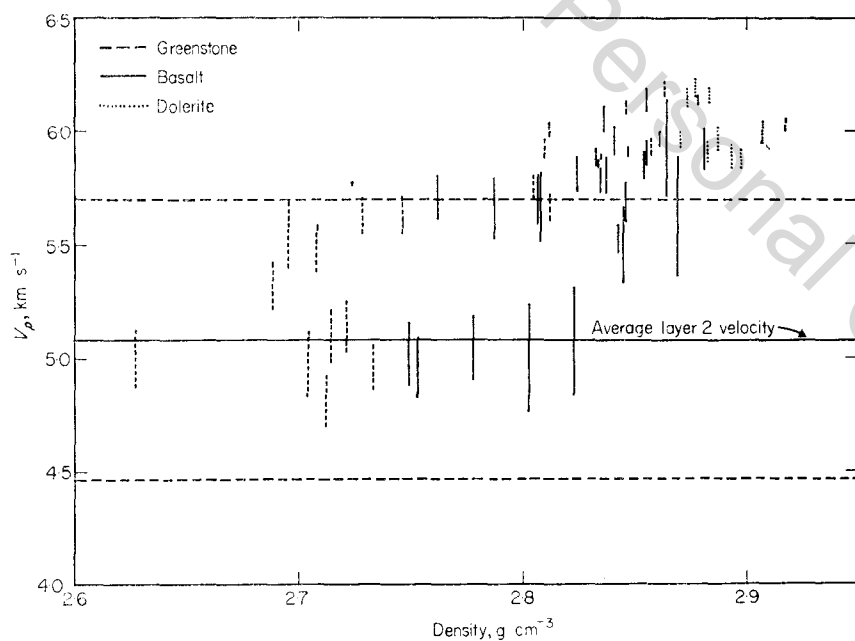


FIG. 2. Compressional wave velocities between 0.2 and 0.6 kb as a function of bulk densities (Table 2) and average layer 2 velocity after Raitt (1963). Horizontal dashed lines represent plus and minus one standard deviation of the average layer 2 velocity.

density (0.5 per cent). To facilitate calculation of the errors, V_p and V_s were assumed to be 6 km s^{-1} and 3.5 km s^{-1} respectively. The estimated errors are ± 4 per cent in K and β , ± 3.5 per cent in ϕ , ± 2.5 per cent in μ , ± 7 per cent in λ , ± 6 per cent in σ , and ± 8 per cent in E .

Discussion

Comparisons of seismic velocities with laboratory velocities at appropriate pressures provide information as to possible mineral assemblages of crustal layers and, perhaps most important, can be used to reject many rocks as major crustal constituents. Comparisons of this type must necessarily assume a certain degree of homogeneity in the crustal layers, at least over distances comparable to the path lengths of waves used in seismic refraction investigations. A test of homogeneity can be based on the variability of measured velocities in various crustal regions. With this in mind, we have plotted in Fig. 2 measured compressional wave velocities at pressures between 0.2 and 0.6 kb for the Mid-Atlantic Ridge rocks versus their bulk densities. The average velocity of layer 2 given by Raitt (1963) and the standard deviation of this average are also shown in Fig. 2. Our measurements show that greenstones and basalts similar to those obtained from the Mid-Atlantic Ridge are possible major constituents of layer 2. Velocities for the denser rocks are slightly high, however fracturing in the upper oceanic crust could lower velocities. The standard deviation of the average layer 2 velocity is quite large ($\pm 0.63 \text{ km s}^{-1}$), which suggests heterogeneity in composition. Thus basalt, altered basalt, dolerite and greenstone may all be important constituents of layer 2.

Crustal velocities at the Mid-Atlantic Ridge crest are similar to layer 2 velocities (Talwani *et al.* 1965). The interpretation of gravity and seismic data over the Mid-

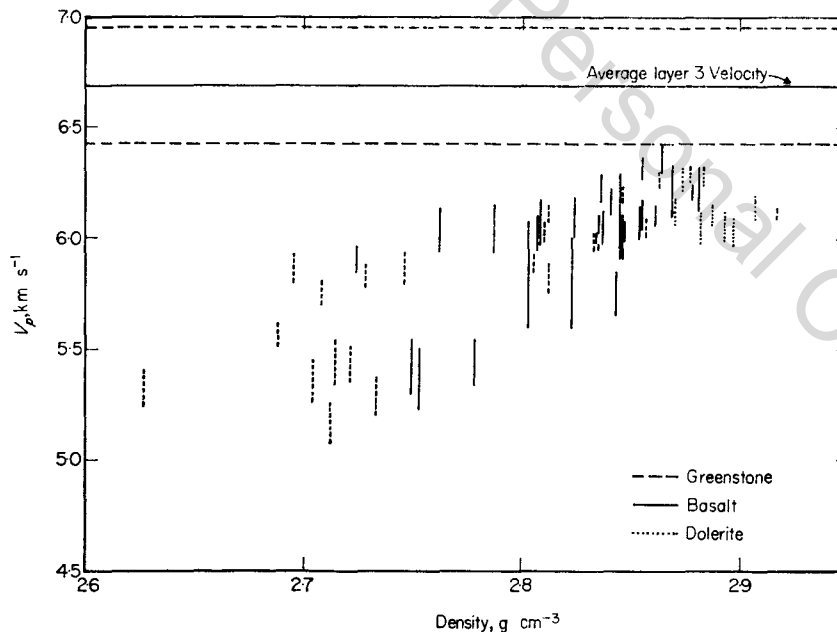


FIG. 3. Compressional wave velocities between 1 and 2 kb as a function of bulk densities (Table 2) and average layer 3 velocity after Raitt (1963). Horizontal dashed lines represent plus and minus one standard deviation of the average layer 3 velocity.

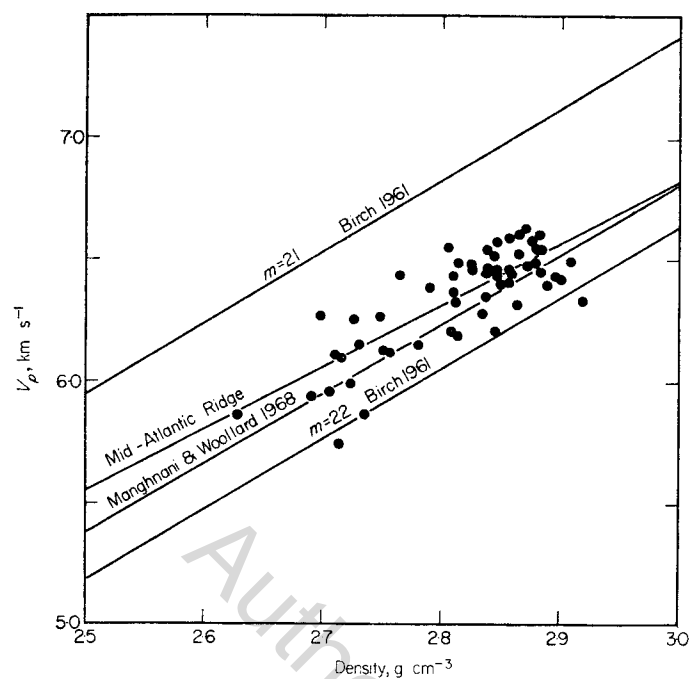


FIG. 4. Compressional wave velocities at 10 kb as a function of bulk densities. Least-squares regression lines of V_p on ρ_b are given for the Mid-Atlantic Ridge samples as well as from previous work.

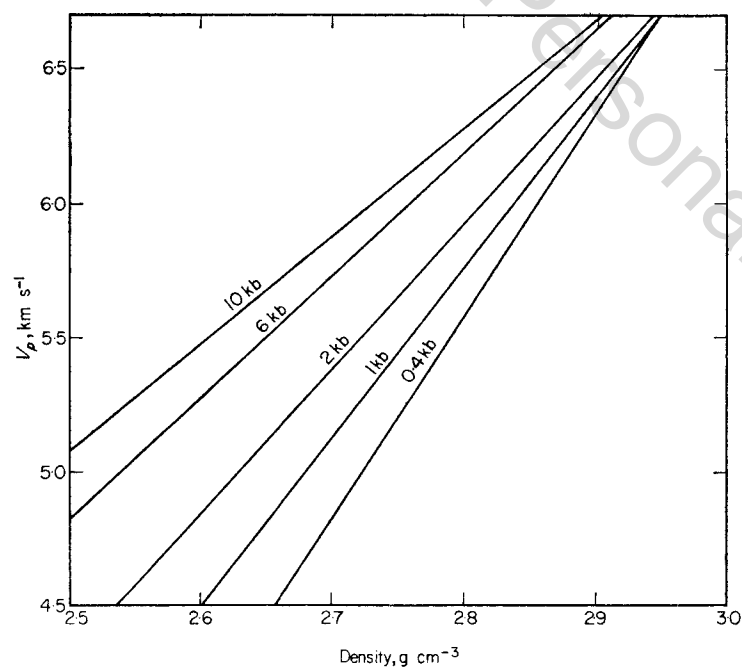


FIG. 5. Least-squares regression lines for ρ_b on V_p for the Mid-Atlantic Ridge specimens.

Atlantic Ridge indicates that layer 3 is absent and the oceanic crust consists only of a thick section of layer 2 (Le Pichon *et al.* 1965). Our measurements suggest that mafic rocks collected along the crest of the Mid-Atlantic Ridge are probably representative of the entire crustal section over the ridge axis.

Layer 3 velocities are relatively uniform (Raitt 1963). This strongly suggests that there is little variability in lower oceanic crustal composition. In Fig. 3 are plotted compressional wave velocities at pressures from 1 to 2 kb versus bulk densities from the data in Table 2. Raitt's average layer 3 velocity and the standard deviation are also shown in Fig. 3. It appears that oceanic basalts, chlorite-rich greenstones, and dolerites cannot be abundant in layer 3. Compressional wave velocity measurements by Christensen (1970) for several relatively high grade epidote-rich continental greenstones are, however, within the range of reported layer 3 velocities.

Perhaps the most interesting aspect of the elastic constants is the behaviour of σ with increasing pressure. The other elastic constants and the velocities show changes of 10 per cent or more in going from 0.4 to 10 kb. The change in σ , however, is much less, the greatest change being for the altered basalt (7 per cent). Since much of the change in elastic properties up to 10 kb may be attributed to closure of cracks, σ may be a very valuable parameter for distinguishing rock types on the basis of elastic properties, particularly at low pressures or in instances where the state of porosity is unknown.

Density-velocity relations

A number of studies (e.g., Birch 1961; Manghnani & Woollard 1968) have been directed toward interpretation of velocity data in terms of density, one aim being a velocity-density relation by which velocities of seismic waves may be used to determine densities for gravity models. The plot of V_p versus ρ_b in Fig. 4 shows the data points as well as the least-square regression line of V_p on ρ_b at 10 kb for the 57 cores of rock

Table 5
Regression line parameters

Pressure (kb)	<i>n</i>	$V_p = a + b\rho_b$		$S_{(V_p, \rho_b)}$ (km s ⁻¹)	<i>r</i>	<i>r</i> ² %
		<i>a</i> (km s ⁻¹)	<i>b</i> ($\frac{\text{km s}^{-1}}{\text{g cm}^{-3}}$)			
0.4	57	-6.16	4.21	0.25	.75	56
1.0	57	-4.63	3.73	0.19	.78	62
2.0	57	-3.70	3.45	0.17	.80	64
6.0	57	-1.70	2.83	0.15	.79	62
10.0	57	-0.76	2.53	0.13	.79	62

Pressure (kb)	<i>n</i>	$\rho_b = a + b V_p$		$S_{(\rho_b, V_p)}$ (g cm ⁻³)	<i>r</i>	<i>r</i> ² %
		<i>a</i> (g cm ⁻³)	<i>b</i> ($\frac{\text{g cm}^{-3}}{\text{km s}^{-1}}$)			
0.4	57	2.06	0.132	0.044	.75	56
1.0	57	1.85	0.165	0.041	.78	62
2.0	57	1.71	0.184	0.040	.80	64
6.0	57	1.44	0.219	0.041	.79	62
10.0	57	1.24	0.248	0.040	.79	62

n = number of data points

$S_{(V_p, \rho_b)}$ = standard error of estimate of V_p on ρ_b

$S_{(\rho_b, V_p)}$ = standard error of estimate of ρ_b on V_p

r = correlation coefficient

*r*² = coefficient of determination

from the Mid-Atlantic Ridge. Birch's (1961) least-square fits for mean atomic weights 21 and 22 and Manghnani & Woollard's (1968) least-square fit for 8 cores of basalt are given for comparison. The scatter in our data points yields a correlation coefficient of 0.79, and 62 per cent of the variation in V_p is accounted for by the variation in ρ_b . The smaller slope of our line as compared to the other lines is probably due in part to the hydrous greenstones which have lower mean atomic weights (hence higher velocities) than basalts of similar density. This may also be seen among the higher density rocks, where greenstones tend to have slightly higher velocities than basalts of the same density. Since greenstones predominated among the lower density rocks, the line is shifted toward higher velocities at the low density end, leading to a smaller slope for the regression line. Mean atomic weights calculated from chemical analyses of Melson *et al.* (1968) lie between 21 and 22.

Fig. 5 shows least-square regression lines of ρ_b on V_p for pressures of 0.4, 1.0, 2.0, 6.0 and 10 kb. These lines have steeper slopes than regression lines of V_p on ρ_b . The difference in slopes is due to the lack of perfect linear correlation between V_p and ρ_b (assuming constant mean atomic weight). The lines decrease in slope continuously with increasing pressure. These lines are the appropriate lines to use for estimating ρ_b from V_p using our data. Such estimation should be done cautiously, since the mean atomic weight is a definite factor to be considered and the slope and position of a velocity-density line will be affected by a systematic variation of mean atomic weight in the data points.

Acknowledgments

We are indebted to Drs Tj. H. van Andel and G. A. Thompson for contributing the valuable samples for this investigation. Technical support by K. V. Campbell, P. Lage and M. Mulcahey is gratefully acknowledged. Financial support was provided by National Science Foundation grant GA-1461.

Department of Geological Sciences,
University of Washington,
Seattle, Washington 98105.

References

- Andel, Tj. H. van, Bowen, V. T., Siever, R. & Sachs, P. L., 1965. *Science*, **148**, 1214.
 Andel, Tj. H. van & Bowen, C. O., 1968. *J. geophys. Res.*, **73**, 1279.
 Birch, F., 1958. *Contributions in Geophysics*, p. 158, Pergamon Press Ltd, Oxford.
 Birch, F., 1960. *J. geophys. Res.*, **65**, 1083.
 Birch, F., 1961. *J. geophys. Res.*, **66**, 2199.
 Christensen, N. I., 1965. *J. geophys. Res.*, **70**, 6147.
 Christensen, N. I., 1966a. *J. geophys. Res.*, **71**, 3549.
 Christensen, N. I., 1966b. *J. geophys. Res.*, **71**, 5921.
 Christensen, N. I., 1968. *Pacific Sci.*, **22**, 41.
 Christensen, N. I., 1970. *Bull. geol. Soc. Am.*, **81**, 905.
 Dortman, N. B. & Magid, M. Sh., 1969. *Internat. geol. Rev.*, **11**, 517.
 Gutenberg, B., 1955. *Spec. Pap. geol. Soc. Am.*, **62**, 19.
 Gutenberg, B., 1959. *Physics of the Earth's Interior*, Academic Press, New York.
 Hill, M. N., 1957. *Progr. phys. chem. Earth*, **2**, 129.
 Kanamori, H. & Mizutani, H., 1965. *Bull. earthquake Res. Inst., Tokyo Univ.*, **43**, 173.
 Le Pichon, X., Houtz, R. E., Drake, C. L. & Nafe, J. E., 1965. *J. geophys. Res.*, **70**, 319.
 Manghnani, M. H. & Woollard, G. P., 1968. *Mono. Am. geophys. Un.*, No. **12**, 501.

- Melson, W. G. & van Andel, Tj. H., 1966. *Marine Geol.*, **4**, 165.
- Melson, W. G., Thompson, G. & van Andel, Tj. H., 1968. *J. geophys. Res.*, **73**, 5925.
- Nur, A. & Simmons, G., 1969. *Earth Planet. Sci. Letters*, **7**, 183.
- Raitt, R. W., 1956. *Bull. geol. Soc. Am.*, **67**, 1623.
- Raitt, R. S., 1963. *The Sea*, Vol. **3**, p. 85, Interscience, New York.
- Simmons, G., 1964. *J. geophys. Res.*, **69**, 1123.
- Talwani, M., Le Pichon, X. & Ewing, M., 1965. *J. geophys. Res.*, **70**, 341.
- Thompson, G., Melson, W. G. & Bowen, V. T., 1969. *Trans. Am. geophys. Union*, **50**, 211.

Author's Personal Copy